UNITED STATES AIR FORCE RESEARCH LABORATORY

APPLICATION OF A NYSTROM METHOD TO SOLVING 3-D ELECTOMAGNETIC INTERIOR SCATTERING PROBLEMS

Sherwood Samn

HUMAN EFFECTIVENESS DIRECTORATE
DIRECTED ENERGY BIOEFFECTS DIVISION
BIOMECHANISM AND MODELING BRANCH
2503 Gillingham Drive, Building 175E
Brooks Air Force Base TX 78235-5102

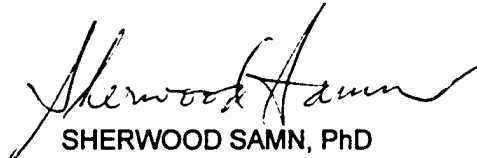July 1998

19980809915 125

NOTICES

This report is published in the interest of scientific and technical information exchange and does not constitute approval or disapproval of its ideas or findings.

Using Government drawings, specifications, or other data included in this document for any purpose other than Government procurement does not in any way obligate the US Government. The fact that the Government formulated or supplied the drawings, specifications, or other data does not license the holder or any other person or corporation; or convey any rights or permission to manufacture, use, or sell any patented invention that may relate to them.

The Office of Public Affairs has reviewed this technical report, and it is releasable to the National Technical Information Service, where it will be available to the general public, including foreign nationals.

This technical report has been reviewed and is approved for publication.

SHERWOOD SAMN, PhD
Project Scientist

RICHARD L. MILLER, PhD
Chief, Directed Energy Bioeffects Division

1. AGENCY USE ONLY (Leave blank)	2. REPORT DATE July 1998	3. REPORT TYPE AND DATES COVERED Interim Report – August 1997 – January 1998

4. TITLE AND SUBTITLE Application of a Nystrom Method to Solving 3-D Electromagnetic Interior Scattering Problems	5. FUNDING NUMBERS PE – 62202F PR – 7757 TA – B4 WU – 02
6. AUTHOR(S) Sherwood Samn	

7. PERFORMING ORGANIZATION NAME(S) AND ADDRESS(ES) Air Force Research Laboratory (AFMC) Human Effectiveness Directorate Directed Energy Bioeffects Division Biomechanism and Modeling Branch 2503 Gillingham Drive, Building 175E Brooks Air Force Base TX 78235-5102	8. PERFORMING ORGANIZATION REPORT NUMBER AFRL-HE-BR-TR-1998-0048

9. SPONSORING/MONITORING AGENCY NAME(S) AND ADDRESS(ES)	10. SPONSORING/MONITORING AGENCY REPORT NUMBER

11. SUPPLEMENTARY NOTES

12a. DISTRIBUTION/AVAILABILITY STATEMENT Approved for public release; distribution is unlimited.	12b. DISTRIBUTION CODE

13. ABSTRACT (Maximum 200 words)

In studying interior scattering problems of electromagnetic waves in biological systems, it is natural to consider finite inhomogeneous models in 3-space. With the advent of ever-increasing computing power and noval computer architecture for parallel processing, integral equation formulations of the problem have become viable alternatives to more traditional finite difference or finite element approaches. This report describes a generalization of the classical Nystrom Method to solving 3-D electromagnetic interior scattering problems using an iterated integral method.

14. SUBJECT TERMS Electromagnetics Iterated Integral Inhomogeneity Nystrom Method Integral Equation	15. NUMBER OF PAGES 20
	16. PRICE CODE

17. SECURITY CLASSIFICATION OF REPORT Unclassified	18. SECURITY CLASSIFICATION OF THIS PAGE Unclassified	19. SECURITY CLASSIFICATION OF ABSTRACT Unclassified	20. LIMITATION OF ABSTRACT UL

Contents

Application of a Nyström Method to Solving 3-D Electromagnetic Interior Scattering Problems

INTRODUCTION

The impetus of our research is electromagnetic (EM) dosimetry. We are interested in determining the distribution of electromagnetic field strength inside a human organ or even the whole body in presence of an externally generated electromagnetic field. This field can come, for example, from a cellular telephone and one is interested in assessing its biological effects. Mathematically, this is a problem of an interior scattering problem where one solves the Maxwell's Equations for an induced field inside a finite body.

For our particular interest here, we are interested in the simple case in which the external source can be modeled as a plane wave and for frequencies in the microwave range.

The interior scattering problem is a classical problem and many solution methods have been proposed. One popular class of methods is the finite-difference time domain (FDTD) methods in which the Maxwell's Equations are discretized directly and solved [5, 12]. Another class of methods, just as popular as FDTD, is Integral Equation (IE) Methods [7]. Here Maxwell's Equations are cast into integral equations and solved using, for example, the Method of Moments (MM) [4].

In this work, we have concentrated on the IE approach. However, instead of using the Method of Moments (MM), we used a variant of the Nyström Method. The Nyström method is more direct and does not require approximating the sought field using basis functions as in MM. The merit of the Nyström Method as a tool to solve electromagnetic scattering problems is rather controversial. There are some who have reported success with this method [2, 13], but others did not [1]. One of the goals of our research is to determine for ourselves the merit of one variant of this method. We believe our approach is new.

1

FORMULATION

In the integral equation formulation the field $\mathbf{E}(\mathbf{r})$ (we assume the time-harmonic case with time factor $e^{-j\omega t}$) is written as the sum of the incident field $\mathbf{E}^i$ and the scattered field $\mathbf{E}^s$:

$$\mathbf{E}(\mathbf{r}) = \mathbf{E}^s(\mathbf{r}) + \mathbf{E}^i(\mathbf{r}) \tag{2.1}$$

where the scattered field $\mathbf{E}^s$ is given by [9]

$$\mathbf{E}^s(\mathbf{r}) = (\mathbf{I} + \frac{1}{k_o^2}\nabla\nabla\cdot)\int_V g(\mathbf{r},\mathbf{r}')\,\mathbf{F}(\mathbf{r}')\,dV' \tag{2.2}$$

where

$$
\begin{aligned}
\mathbf{F}(\mathbf{r}) &= \tau(\mathbf{r})\,\mathbf{E}(\mathbf{r}) \\
\tau(\mathbf{r}) &= k^2(\mathbf{r}) - k_o^2 \\
g(\mathbf{r},\mathbf{r}') &= \frac{e^{jk_o r}}{4\pi r} \\
r &= |\,\mathbf{r} - \mathbf{r}'\,|
\end{aligned}
$$

The two "differentiations" outside the integral in equation (2.2) are numerically undesirable. It would be desirable to move the two "differentiations" through the integral and obtain

$$
\begin{aligned}
\mathbf{E}^s(\mathbf{r}) &= \int_V \bar{\mathbf{G}}(\mathbf{r},\mathbf{r}')\,\mathbf{F}(\mathbf{r}')\,dV' \\
\bar{\mathbf{G}}(\mathbf{r},\mathbf{r}') &= (\mathbf{I} + \frac{1}{k_o^2}\nabla\nabla\cdot)\,g(\mathbf{r},\mathbf{r}')
\end{aligned}
$$

Unfortunately, this is mathematically incorrect, as the resulting integral is now divergent. One can, however, still move one "differentiation" safely through the integral. In MM, one can eliminate the remaining "differentiation" outside the integral by moving it over to the testing functions [3]. Without using the MM, we can move it through the integral only indirectly, resulting in a more complicated equation. In particular, by avoiding the singularity and applying "integration by parts" and the divergence theorem several times, one can arrive at the following equivalent formulation (assuming $\mathbf{F}$ satisfies a local Hölder condition):

$$
\begin{aligned}
\mathbf{E}^s(\mathbf{r}) &= \int_V g(\mathbf{r},\mathbf{r}')\,\mathbf{F}(\mathbf{r}')\,dV' \\
&+ \frac{1}{k_o^2}\int_{V-V_e(\mathbf{r})} \nabla'\nabla' g(\mathbf{r},\mathbf{r}')\,\mathbf{F}(\mathbf{r}')\,dV'
\end{aligned}
$$

2

$$+ \; \frac{1}{k_o^2} \; \int_{V_e(\mathbf{r})} \; \nabla' \nabla' g(\mathbf{r}, \mathbf{r}') \; (\mathbf{F}(\mathbf{r}') - \mathbf{F}(\mathbf{r})) \; dV'$$

$$+ \; \frac{1}{k_o^2} \; \int_{\partial V_e(\mathbf{r})} \; \nabla' g(\mathbf{r}, \mathbf{r}') \hat{n}' \; dS' \; \mathbf{F}(\mathbf{r}) \tag{2.3}$$

where $V_e(\mathbf{r})$ is a sub-volume of V containing $\mathbf{r}$.

Two common methods for evaluating equation (2.3) exist, depending on the choice of $V_e(\mathbf{r})$. By decomposing the body V into finite volume elements (e.g. tetrahedra), one can naturally take $V_e(\mathbf{r})$ to be the volume element that contains $\mathbf{r}$ [14].

The other common method allows $V_e(\mathbf{r})$ to vanish around $\mathbf{r}$. This leads to an apparently simpler integral equation [14]. However, it requires the evaluation of a principal-value integral, which is numerically difficult.

The approach we have taken here is to let $V_e(\mathbf{r}) = V$. This leads to the equation

$$
\begin{aligned}
\mathbf{E}^{\mathbf{s}}(\mathbf{r}) \; &= \; \int_V \; g(\mathbf{r}, \mathbf{r}') \; \mathbf{F}(\mathbf{r}') \; dV' \; + \frac{1}{k_o^2} \; \int_{\partial V} \; \nabla' g(\mathbf{r}, \mathbf{r}') \hat{n}' \; dS' \; \mathbf{F}(\mathbf{r}) \\
&+ \; \frac{1}{k_o^2} \; \int_V \; \nabla' \nabla' g(\mathbf{r}, \mathbf{r}') \; (\mathbf{F}(\mathbf{r}') - \mathbf{F}(\mathbf{r})) \; dV' \\
&= \; \bar{\mathbf{A}}(\mathbf{r}) \, \mathbf{F}(\mathbf{r}) + \int_V \; \bar{\mathbf{G}}(\mathbf{r}, \mathbf{r}')(\mathbf{F}(\mathbf{r}') - \mathbf{F}(\mathbf{r})) \; dV'
\end{aligned}
\tag{2.4}
$$

where

$$\bar{\mathbf{A}} = \frac{1}{k_o^2} \; \int_{\partial V} \; \nabla' g(\mathbf{r}, \mathbf{r}') \hat{n}' \; dS' \; + \int_V \; g(\mathbf{r}, \mathbf{r}') \; \bar{\mathbf{I}} \; dV'$$

For a specified $\mathbf{r}$, $\bar{\mathbf{A}}$ is completely known, so it can be accurately estimated.

THE NYSTRÖM METHOD

The Nyström Method assumes the integrals in Equations (2.3 or 2.4) can be approximated well by quadrature formulas using N quadrature points $\{\mathbf{r_i}\}_{i=1}^N$. If Equation (2.1) is also evaluated at these same N points, then one obtains a linear system of N vector equations in the N unknown vectors $\{\mathbf{E}(\mathbf{r_i})\}_{i=1}^N$. Inverting this system will yield the values of $\{\mathbf{E}(\mathbf{r_i})\}$, which in turn can be used to estimate the value of the electromagnetic field $\mathbf{E}(\mathbf{r})$ at any other point $\mathbf{r}$ by using a discretized version of equation (2.1).

The main sources of errors in the Nyström method as formulated here are (1) the singularity of some of the integrals, (2) the numerical approximation of the integrals, and (3) the possible ill-conditioning of the system of equations. We will only address the first two sources of errors in the following.

3

In some of our previous numerical experiments [8] with equation (2.3) using MM, we have encountered some numerical difficulties. Unsatisfactory results were observed whenever the contrast τ is large or when more tetrahedra were used to represent the volume V. This could be caused by a multitude of things including the improper handling of the singularity, the poor choice of basis functions and/or testing functions, inappropriate dot-product, low-order numerical integration, sub-optimal choice of tetrahedra, or poor meshing in general.

By using the Nyström method, we eliminate the need to consider basis/testing functions and to some extent (as we will we see later) meshing.

SINGULARITY: A 1-D TEST

Equation (2.4) is theoretically correct if we assume $\mathbf{F}$ satisfies a local Hölder condition so that the integral

$$\int_V \nabla'\nabla'g(\mathbf{r},\mathbf{r}')\,(\mathbf{F}(\mathbf{r}') - \mathbf{F}(\mathbf{r}))\,dV' \tag{3.5}$$

is convergent, despite the singularity at $\mathbf{r}$. Since $\mathbf{F}$ is unknown, one way to incorporate this assumption on $\mathbf{F}$ (and we must) into a numerical quadrature is to assume the contribution of the singular point $\mathbf{r}$ to the volume integral in Equation (3.5) is negligible. More precisely, the volume integral over a sufficiently small volume surrounding $\mathbf{r}$ is negligible. This is basically a reiteration of the fact that Equation (3.5) is convergent when $\mathbf{F}$ satisfies a local Hölder condition.

To get an idea of the consequence of this assumption, we studied the following 1-D problem analogous to the actual 3-D problem described in Equation (2.4).

$$\begin{aligned}
\beta\,f(x) \quad &- \quad \left(\int_0^1 g(x,x')\,f(x')\,dx'\right. \\
&+ \quad \alpha\,\frac{d^2}{dx^2}\int_0^1 g(x,x')\,f(x')\,dx' = u^{inc}(x)
\end{aligned} \tag{3.6}$$

where typically,

$$\begin{aligned}
f(x) &= \tau(x)\,u(x), & \tau(x) &= k^2(x) - k_o^2 \\
\beta(x) &= \frac{1}{\tau(x)}, & \alpha &= \frac{1}{k_o^2}
\end{aligned}$$

Furthermore, we assume (again motivated by the actual 3-D problem)

$$\begin{aligned}
g(x,x') &= g(x,x') \\
g_x(x,x') &= -g_{x'}(x,x')
\end{aligned}$$

4

$$\int_0^1 g(x, x') \, dx' \qquad \text{is convergent}$$

$$\lim_{\epsilon \to 0} \int_{x-\epsilon}^{x+\epsilon} g_x(x, x') \, dx' \qquad \text{exists}$$

$$\int_0^1 g_{x'x'}(x, x') \, dx' \qquad \text{is divergent} \qquad (3.7)$$

Analogous to the 3D case, this equation can be reformulated as

$$
\begin{aligned}
[\beta \quad - \quad & r(x) - \int_0^1 g(x, x') \, dx'] \, f(x) - \int_0^1 [g(x, x') \\
+ \quad & \alpha \, g_{x'x'}(x, x')] \, (f(x') - f(x)) \, dx' \\
= \quad & u^i(x)
\end{aligned}
\qquad (3.8)
$$

where

$$r(x) = \alpha[g_x(x, 0) - g_x(x, 1)]$$

A function $g(x, x')$ that has all the properties listed in (3.7) is

$$g(x, x') = \mid x - x' \mid \, (\ln \mid x - x' \mid -1) \qquad (3.9)$$

This is the function we have used.

In the Nyström Method we used, the N quadrature points (and corresponding weights) chosen to evaluate the integrals in the IE are the those determined by the Gauss-Legendre quadrature points (GLQPs) [10] on [0,1]. More sophisticated choice of quadrature points (and weights) that depends on the singularity in question could have been designed [6], but was not done in this exploratory study.

The sum of the weights is always equal to the length of the integration interval. We might view the GLQPs as a partition of [0,1] into sub-intervals each of which is centered around a GLQP and whose length is equal to the corresponding weight. The assumption that the solution satisfies a local Hölder condition implies that the contribution from (2.4) is finite and negligible if the norm of the partition is small. In short, we may make the following approximation:
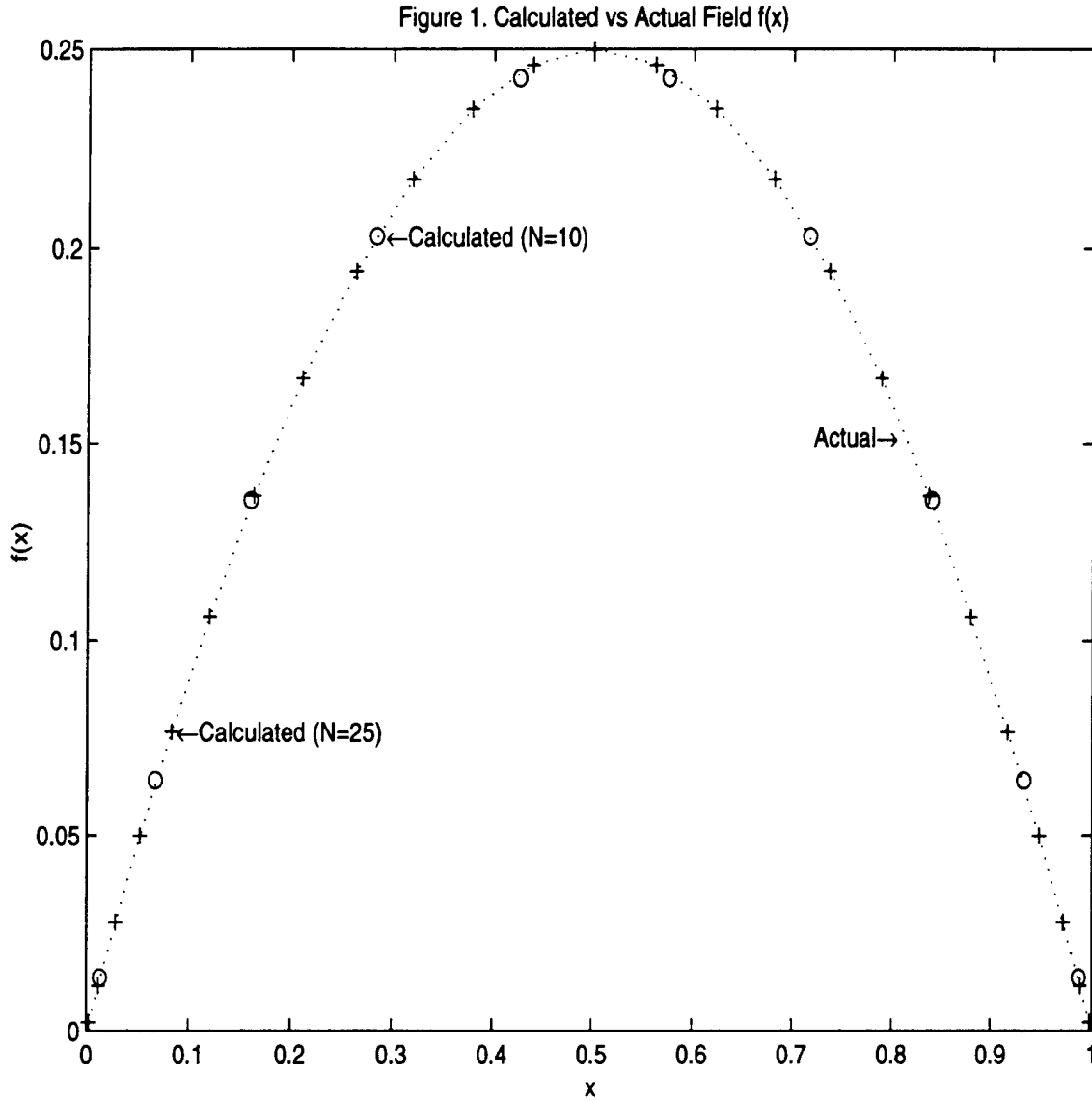
$$
\begin{aligned}
\int_0^1 & g_{xx}(x_i, x') \, (f(x') - f(x_i)) \, dx' \\
& = \sum_{j \neq i} w_j \, g_{xx}(x_i, x_j) \, (f(x_j) - f(x_i))
\end{aligned}
\qquad (3.10)
$$

5

We generated simulated data by using the function

$$f(x) = x(1 - x) \qquad\qquad (3.11)$$

to calculate an "incident wave".

The results are shown in Figure 1. It shows the actual solution and the calculated solution for $N = 10$ and $N = 25$.

Figure 1. Calculated vs Actual Field f(x)

For this example, the calculated solution approximates well the actual solution even when N is as low as 25. The "relative permittivity" here is 3.

AN ITERATED INTEGRAL METHOD

The apparent success of the 1-D analog problem holds out hope that the same might be true for the actual 3-D problem. Since the formulation of the problem in the 1-D case is identical to that in the 3-D case, it remains only to choose a 3-D integration method to complete the transition from 1-D to 3-D.

The following is a brief summary of our experimenting with different possible 3-D integration methods, cumulating in the Iterated Integral Method (IIM).

A. Integration on Tetrahedra

Methods of integration over tetrahedra abound in the literature. (Notably the classic work of Stroud.) We have implemented some of these methods by approximating the body in question by a family of tetrahedra or a family of curvilinear tetrahedra (for a better approximation) and using different integration formulas (differing in orders) on each tetrahedron or curvilinear tetrahedron (after appropriate transformation.) The results are mixed but generally disappointing. We remark in passing that by increasing the order of the method of integration on each tetrahedron, one invariably increases the number of integration points in each tetrahedron and thereby increases the number of unknowns and hence the size of the system matrix. The effect of increasing the order of the method of integration on the accuracy of the final solution is not clear at this time. Our preliminary studies also seem to indicate an increase in condition numbers of the system matrices as the order of integration is increased. This suggests a subtle difference between numerical integration of a known function and that of an unknown function (as in solving an IE): merely using a more accurate numerical integration method does not necessarily yield a more accurate IE solver.

B. Extrapolation

One way to increase the order of the integration method without increasing the number of integration points is to use points outside the integration domain. So, instead of using only points of integration within a tetrahedron, we can also use a pre-specified number of points in neighboring tetrahedra. We have implemented one such method. In this method, the set of integration points will consist of the "centers" of all the tetrahedra in the system. (This is different from the 1-D case where the integration points are not predefined, but are chosen to optimize the order of the integration method.) For each tetrahedron, T, we picked a pre-specified number of nearest (independent) centers as the integration points for this tetrahedron, i.e., weights associated with these selected integration points and for this tetrahedron will be calculated so that certain moments are integrated exactly on the tetrahedron T.

We observed that the weights generated by this method are often negative and are susceptible to round off errors as well as errors incurred by approximating the given body by tetrahedra.

We did not observe a significant improvement over the previous methods in which only interior quadrature points are used in the quadrature formulas for approximating integrals over tetrahedra.

C. Iterated Integral Method (IIM)

Under the assumption that F satisfies a local Hölder condition, all integrals in Equation 2.4 are absolutely convergent and we can evaluate them as iterated integrals (Fubini's Theorem.) Consequently, since each iterated (volume) integral is made up of three separate 1-D integrals, one can easily generate, for example, 3-D Gauss-Legendre quadrature points and weights from 1-D Gauss-Legendre quadrature points and weights. As long as the material boundaries (internal and external) of the body in question are known, the Gaussian points and weights can be calculated rather straightforwardly. In particular, no explicit discretization (meshing) of the body is required. This can be a significant advantage this method has over the more conventional methods in which meshing is required, as meshing is sometimes the Achilles' heels of these methods.

A 3-D TEST OF NYSTRÖM METHOD USING IIM

We tested the Nyström Method using IIM (NM-IIM) on an integral equation identical in form to equation (2.1) wherein equation (2.4) is used for the scattered field. However, the test problem was chosen to have no singularity, as we were only interested, at the initial stage, in testing the NM-IIM in a setting insulated from other factors that may complicate the problem.

The irradiated body is a 5 cm sphere. For simplicity, we used

$$
\begin{aligned}
\mathbf{E(r)} &= [x, y, z] \\
g(\mathbf{r}, \mathbf{r'}) &= (x - x')^4 + (y - y')^4 + (z - z')^4
\end{aligned}
$$

in the equation

$$
\begin{aligned}
\bar{\mathbf{B}} \, \mathbf{F(r)} &- \int_V \bar{\mathbf{G}}(\mathbf{r}, \mathbf{r'}) \, (\mathbf{F(r')} - \mathbf{F(r)}) \, dV' \\
&= \mathbf{E^{inc}(r)}
\end{aligned}
$$

8

to generate an "incident wave". Here

$$\bar{\mathbf{B}} = a(\mathbf{r})\bar{\mathbf{I}} - \frac{1}{k_o^2} \int_{\partial V} \nabla' g(\mathbf{r},\mathbf{r}')\hat{\mathbf{n}}' \ dS'$$

$$a(\mathbf{r}) = \frac{1}{\tau(\mathbf{r})} - \int_V g(\mathbf{r},\mathbf{r}') \ dV'$$

$$\mathbf{F}(\mathbf{r}) = \tau(\mathbf{r})\mathbf{E}(\mathbf{r})$$

Figure 2 compares the real part of the z-component of the calculated field with that of the actual field along the z-axis. For this simple test, this is just z. Thus, the straight line in Figure 2 is expected.

Figure 2. Actual vs Calculated Re(Ez) (er=52: N=151)
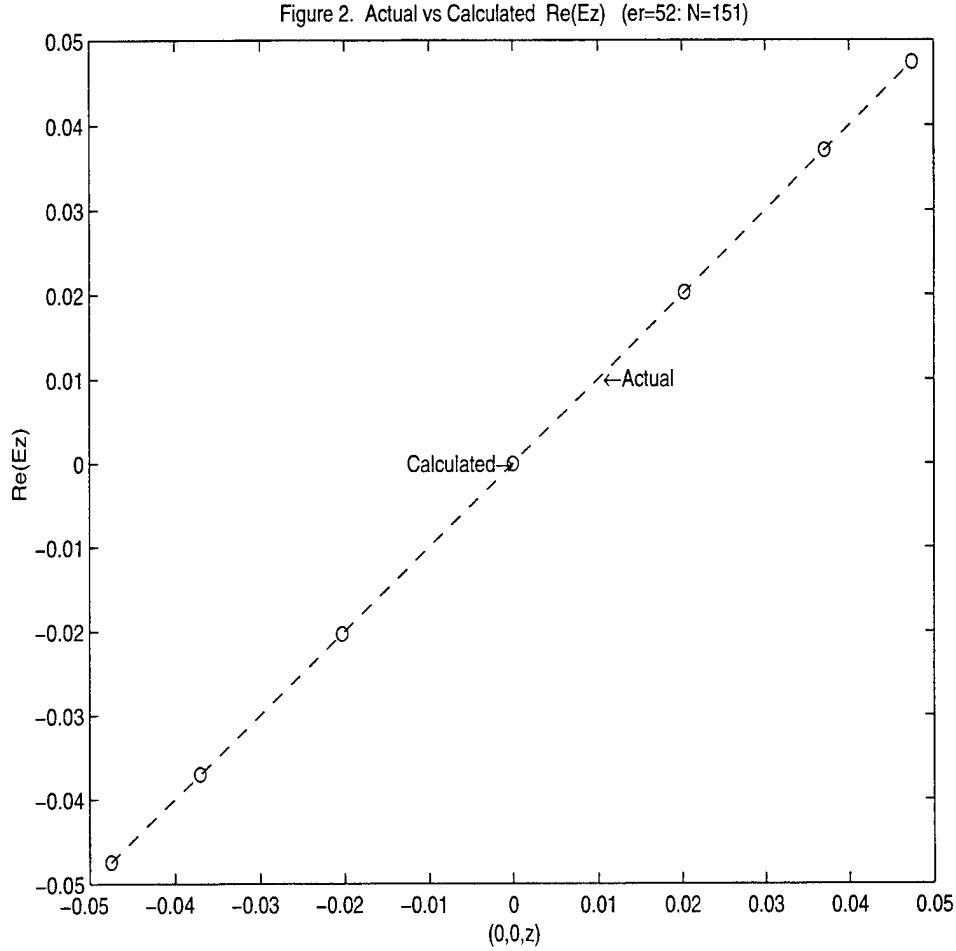
A total of 151 quadrature points in the sphere were picked (by the solver). The "relative permittivity" was chosen to be 52. Judging from this test, albeit simple, the IIM seems to be working.

APPLICATIONS

Finally, we applied the 3D NM-IIM to a realistic problem consisting of a dielectric sphere incident by a 1-GHz plane wave propagating along the z-axis towards positive infinity. The radius of the sphere is 5 (cm) and the conductivity is set to 0.015625 (mhos/m).

A. Homogeneous Sphere

The results of applying NM-IIM to the above problem using differing relative permittivities (ϵ_r) are shown in the Figure 3. It compares the real part of actual x-component of the E field along the z-axis to that calculated by NM-IIM. The dotted lines in the Figure 3 represent the actual (Mie) solutions, one for each relative permittivity. Here $\epsilon_r \approx 1^+, 2^+, 3^+$, and 13^+.

There is generally a fairly good agreement between the actual and the calculated, although again performance noticeably deteriorates with increased relative permittivity or, equivalently, with higher contrasts. The number of quadrature points used for this sphere is 608.

B. An Inhomogeneous Sphere

By manipulating the limits of integration in IIM, the NM-IIM can also be applied to inhomogeneity bodies. More generally, one can vary the grid size (resolution) from one sub-region to another in the body quite straightforwardly.

The Figure 4 shows the result of using NM-IIM on the above sphere using different resolutions in two different sub-regions. The sphere is divided into two sub-regions, an inner sphere and an outer layer. The radius of the inner sphere is 2.5 cm, whereas the complete sphere again has radius 5 cm. The outer layer is chosen to have twice the resolution as that of the inner sphere. We also compare this variable grid case to a uniform grid case. The resolution of the uniform grid is equal to that of the inner sphere of the variable grid case. A total of 151 points is used for the uniform grid case and 612 points for the variable grid case. The relative permittivity is approximately 3. Figure 4 shows the calculated and actual real part of the x-compoenent of the E field along the z-axis of the sphere. Again, the incident plane wave, linearly polarized in the x-direction, is propagating from the negative z-direction. linearly polarized in the x-direction.

Again, the calculated field compares quite well with the theoretical solution and the added resolution in the outer layer has noticeably improved the accuracy of the method.

Figure 3. Calculated Re(Ex) vs Actuals (N=608)

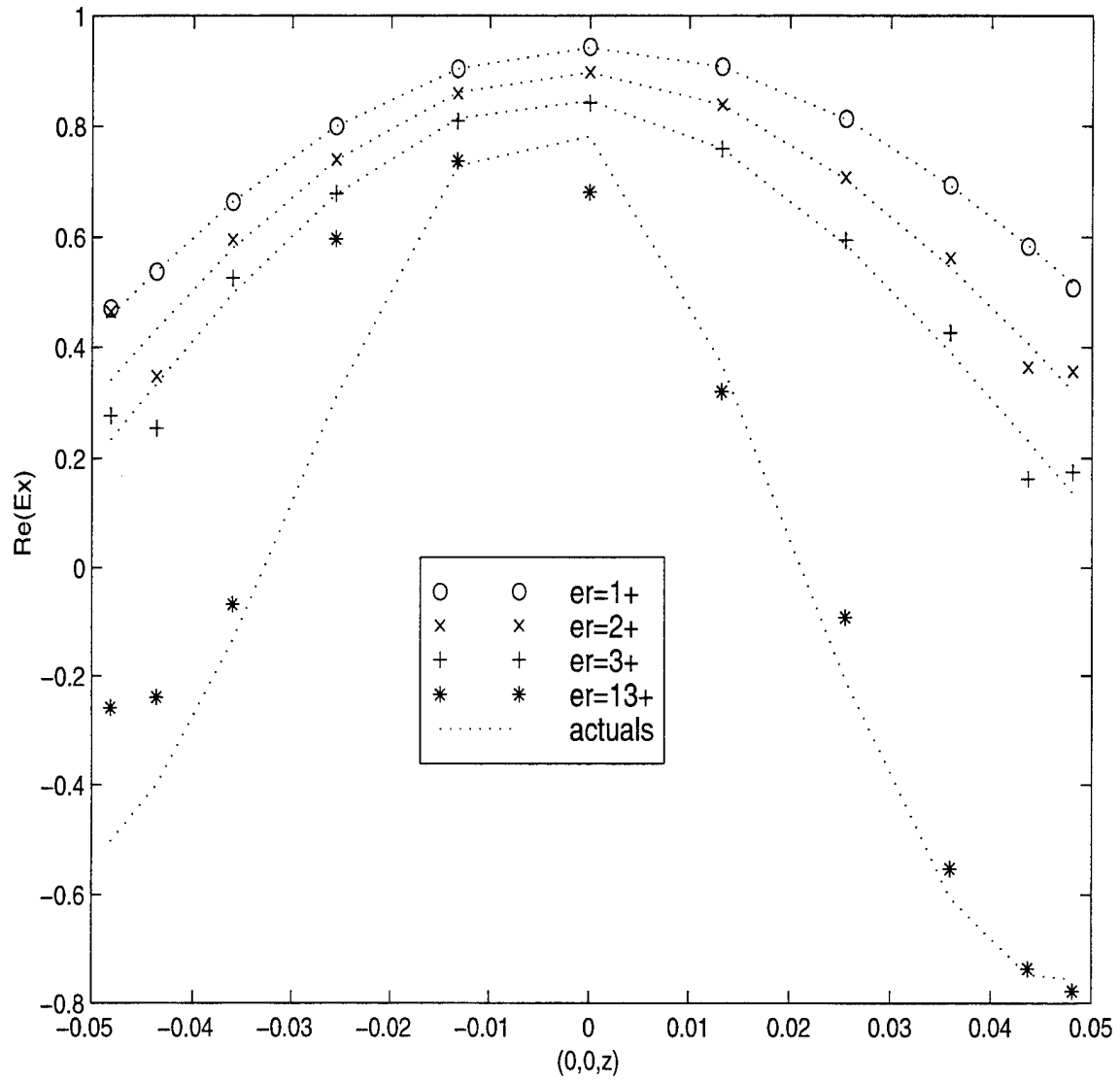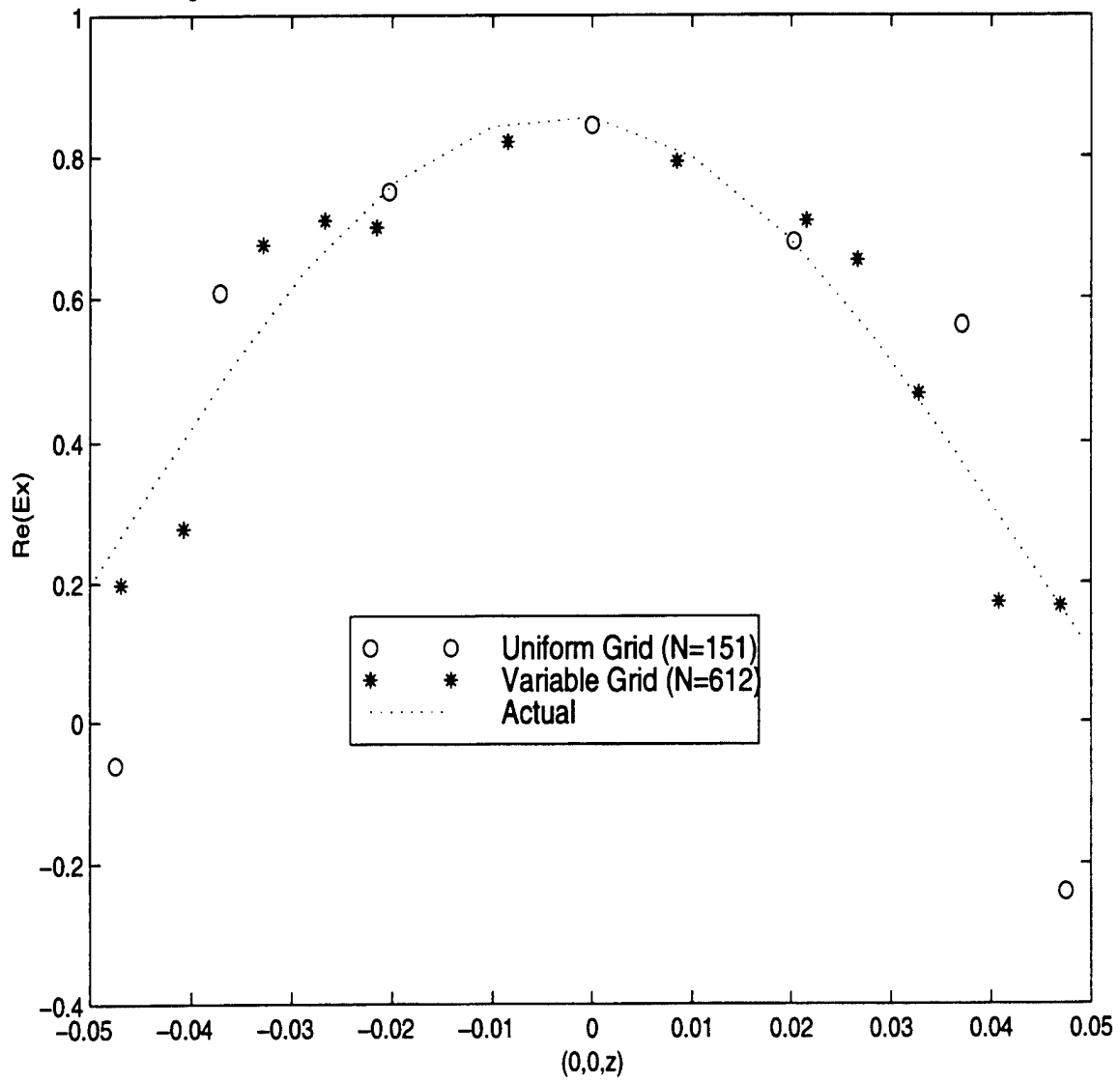Figure 4. Calculated Re(Ex) Using Variable Grid and Uniform Grid vs Actual (er = 3+)

DISCUSSION AND CONCLUSION

The Nyström Method in combination with the Iterated Integral Method (NM-IIM) as implemented here has out-performed other methods that we have previously tried. Because it is "grid-free" and relatively easy to implement, it can easily be used on other geometry (besides spheres) like layered ellipsoids, finite layered cylinders, or even simple human organs.

There is obviously much room for improvement. The first approximation we used in treating the singularity can obviously be improved. The fact that the estimates near the boundary is generally poorer than those in the middle may be consequence of this first approximation. In the neighborhood of a singularity, the integrand is a function of the Jacobian of the unknown $F(r)$. The assumption that this contribution is small may not be appropriate near a boundary.

We should probably use even more sophisticated 1-D Gaussian quadrature formulas that will take better account of the singularity in the problem, similar in flavor to that discussed in [6]. Hopefully, this will then allow us to address problems with even higher contrasts that one routinely encounters in human organs.

A rigorous numerical analysis of NM-IIM is obviously needed. Good performance of a method on test problems only lends credence to the method, but never an absolute proof. The same analysis can invariably lead to improvement of the method.

Finally, as is always the case, we would like to be able to solve more practical and more realistic problems (bigger geometry, higher frequencies, and severer inhomogeneity) and to do so faster. Parallel computing on high performance computers is the most obvious answer. We have just started to explore this possibility.

BIBLIOGRAPHY

[1] M. Bleszynski. (Private communications, 1997)

[2] D. Colton and R. Kress, *Inverse Acoustic and Electromagnetic Scattering Theory*, Springer-Verlag, 1992.

[3] H. Gan and W. C. Chew, *A Discrete BCG-FFT Algortihm for Solving 3D Inhomogeneous Scatterer Problems*, J. Electromag. Waves Appl., vol 9, #10, pp. 1339-1357, 1995.

[4] Harrington, R. F. *Field Computation by Moment Methods*, Robert E. Krieger Publishing Co.,1968.

[5] K. S. Kunz and R. J. Luebbers, *The Finite Difference Time Domain Method for Electromagnetics*, CRC Press, 1993.

[6] J. Ma, V. Rokhlin, and S. Wandzura, *Generalized Gaussian Quadrature Rules for Systems of Arbitrary Functions*, SIAM J. Numer. Anal., Vol 33, No. 3, pp. 971-996, June 1996.

[7] N. Morita, N. Kumagai, and J. R. Mautz, *Integral Equation Methods for Electromagnetics*, Artech House, Inc., 1991.

[8] S. Samn, *Three-Dimensional Electromagnetic Scattering From Arbitrary Inhomogogeneous Objects*, AL/OE-TR-1997-0021, 1997.

[9] S. Samn, *On a Volume Integral Equation Used in Solving 3-D Electromagnetic Interior Scattering Problems*, AL/OE-TR-1997-0121, 1997.

[10] A. H. Stroud and D. Secrest, *Gaussian Quadrature Formulas*, Prentice-Hall, Englewood Cliffs, NJ, 1966.

[11] A. H. Strou. *Approximate Calculation of Multiple Integrals*, Prentice-Hall, Englewood Cliffs, NJ, . .1.

[12] A. Taflove, *Computational Electrodynamics: The Finite-Difference Time-Domain Method,* Artech House, 1995.

[13] S. Wandzura, (Private communications)

[14] J. J. H. Wang, *Generalized Moment Methods in Electromagnetics: Formulation and Computer Solutions of Integral Equations,* John Wilely & Sons, Inc., 1991.